*Acta Polytechnica* **66**(2):209–218, 2026
`https://doi.org/10.14311/AP.2026.66.0209`

# THE IMPACT OF ALKALI OXIDES $NA_2O$ AND $RB_2O$ ON THE PHASE COMPOSITION AND HYDRATION OF $C_3A$

Simona Ravaszová[a,*], Karel Dvořák[a], Andrea Jančíková[a], Michal Křištof[a], Martin Boháč[b]

[a] *Brno University of Technology, Faculty of Civil Engineering, Institute of Technology of Building Materials and Components, Veveří 95, 602 00 Brno, Czech Republic*

[b] *Research Institute for Building Materials, Hněvkovského 65, 617 00 Brno, Czech Republic*

[*] corresponding author: `Simona.Ravaszova@vut.cz`

Abstract. Portland cement clinker contains $C_3A$ as one of its key phases. During firing, it forms a melt that is essential for the formation of $C_3S$ and $C_2S$. Commonly, two polymorphs of $C_3A$ are present: cubic and orthorhombic, and their presence influences the kinetics of cement hydration. This study focused on the effects of $Na_2O$ and $Rb_2O$ dopants on the polymorphic modifications of $C_3A$. It was found that $Na_2O$ in concentrations of 0–2.5 % promotes the formation of the cubic polymorph, while higher concentrations, above 2.5 %, lead to a transition to the orthorhombic polymorph. For $Rb_2O$, incompatibility with calcium was observed, resulting in the formation of new phases and the leaching of rubidium oxide at high firing temperatures. In terms of hydration, samples containing $Na_2O$ exhibited higher reactivity due to the presence of orthorhombic $C_3A$, whereas $Rb_2O$ slowed down hydration, which remains an issue for further research.

Keywords: Tricalcium aluminate, dopants, sodium, rubidium, solid-state synthesis.

## 1. Introduction

Tricalcium aluminate, chemically also denoted as $Ca_3Al_2O_6$ and further abbreviated as $C_3A$, is one of the four main minerals of Portland cement clinker and plays an important role in the early strength development of cement. This clinker mineral is formed by the reaction of calcium and aluminium oxides at high temperatures in a rotary kiln.

From the binary $CaO\text{-}Al_2O_3$ system, it is evident that $C_3A$ melts incongruently at a temperature of 1 542 °C, forming multiple phases with different compositions. $C_3A$ exhibits very high reactivity, significantly influencing the hydration rate of cement. When $C_3A$ comes into contact with water and sulphates, ettringite may form [1, 2].

The typical amount of tricalcium aluminate in Portland cement is around 10 %. To control and potentially slow down the reaction rate of $C_3A$ and delay the overall setting process of Portland cement, finely ground gypsum ($CaSO_4 \cdot 2H_2O$) is added to the clinker [3, 4].

Tricalcium aluminate exists in three polymorphic modifications, which differ in crystal structure depending on temperature, processing conditions (composition), and the presence of foreign ions. In its pure form, $C_3A$ crystallises in a cubic polymorph. In the presence of foreign ions, particularly sodium ($Na^+$), potassium ($K^+$), silicon ($Si^{4+}$), or iron ($Fe^{3+}$), structural changes occur, leading to the formation of other polymorphs: orthorhombic or monoclinic $C_3A$.

The cubic form of $C_3A$ has a unit cell with an edge length of approximately 15.26 Å and contains 64 subcells. Eight of these subcells contain empty rings $(Al_6O_{18})^{18-}$, composed of six $AlO_4$ tetrahedra. The remaining 56 subcells host calcium ions ($Ca^{2+}$), either in the centre or near the edges of these rings. The coordination of $Ca^{2+}$ ions at the edges are octahedral, while in the centre it is irregular, associated with 5 or 6 oxygen atoms. All lattice vectors are of equal length and mutually perpendicular (angle 90°, $\alpha = \beta = \gamma$).

In contrast, the orthorhombic polymorph of $C_3A$ has different lattice parameters ($a \neq b \neq c$), with approximate values: $a = 14.8$ Å, $b = 7.4$ Å, and $c = 6.6$ Å. Although the vector lengths differ, they remain mutually perpendicular (angle 90°) [5, 6].

The formation of different polymorphs is strongly influenced by temperature and the presence of foreign ions, so-called dopants. Among the main dopants is sodium ($Na^+$), which can substitute for calcium ($Ca^{2+}$) ions. This substitution occurs such that one $Ca^{2+}$ ion is replaced by two $Na^+$ ions, one taking the original $Ca^{2+}$ site, and the other occupying a free site in the centre of the $(Al_6O_{18})^{18-}$ ring. This substitution can enhance and stabilise the properties of $C_3A$ polymorphs and to a greater extent, modify their structure. Table 1 below describes the percentage of $Na_2O$ required to form and stabilise the various polymorphic forms [7–9].

Behaviour of $C_3A$ polymorphs in Portland cement:

**Cubic polymorph of $C_3A$** Reacts very rapidly with water at room temperature, leading to fast setting of the resulting cement. Therefore, calcium sulphate ($CaSO_4$) must be added to slow down this reaction and allow the formation of hydration

| $Na_2O$ Content [%] | Polymorphism |
|---|---|
| 0–1 | Cubic I |
| 1–2.4 | Cubic II |
| 2.4–3.7 | Cubic + orthorhombic |
| 3.7–4.6 | Orthorhombic |
| 4.6–5.7 | Monoclinic |

Table 1. Percentage of $Na_2O$ and polymorphic changes of $C_3A$ [4].

products such as ettringite. In commercial Portland cements, this polymorph occurs alone or in combination with the orthorhombic form [10].

**Orthorhombic polymorph of $C_3A$** During the reaction of orthorhombic $C_3A$ with water, the same hydration products form as in the cubic form, both in the presence and absence of $CaSO_4$. However, unlike the cubic form, the orthorhombic polymorph reacts faster with water when $CaSO_4$ is present as compared to pure orthorhombic $C_3A$, making the addition of $CaSO_4$ ineffective. As mentioned earlier, both polymorphs are found in commercial Portland cement either separately or in combination [11, 12].

**Monoclinic polymorph of $C_3A$** As with the orthorhombic form, the monoclinic polymorph also exhibits a faster reaction rate with water in the presence of $CaSO_4$ than the cubic polymorph. Unlike the previous two forms, the monoclinic modification has not been or only very rarely observed in commercial Portland cements. Some studies report that this polymorph can occur in commercial cements and is typically modified by both $Na_2O$ and $K_2O$ [13–15].

Sodium is the most common foreign ion known to influence and alter the structure of $C_3A$, leading to the formation of different polymorphic modifications. This issue was addressed in a study by Ostrowski and Zelazny [15], who investigated not only how the structure of $C_3A$ changes with a lower $Na_2O$ content (from 0 % to 5.2 %), but also what occurs when the $Na_2O$ content exceeds 5.2 %, a threshold beyond which free calcium oxide (CaO) begins to separate.

For the experiment, synthesised crystalline forms of solid solutions of $Na_2O$ in $C_3A$, $C_{12}A_7$, and CA were used. These solid solutions were formed at 1 250 °C through isomorphic substitution of calcium ions with sodium ions. The researchers also attempted to synthesise hypothetical compounds, namely $NC_8A_3$ and $N_2C_3A_5$.

The results of this study confirmed that within the range of 0–5.2 % $Na_2O$ in the $C_3A$ solid solution, different polymorphic modifications formed progressively in the order:

- Cubic (1.8–2.5 wt. % $Na_2O$),
- orthorhombic (3.5–4.2 wt. % $Na_2O$),
- monoclinic (5.2 wt. % $Na_2O$).

At $Na_2O$ concentrations above 5.2 wt. %, the $C_3A$ structure transformed from the original monoclinic polymorph into sodium aluminate ($NaAlO_2$) and free CaO.

They also found that doping calcium aluminate (CA) with sodium ions up to 10 wt. % $Na_2O$ increased the content of $C_{12}A_7$ and $N_2C_3A_5$ phases. XRD analysis further revealed that in the CA-$Na_2O$ system, a $C_3A$-$Na_2O$ solid solution was formed, where at 20 wt. % $Na_2O$, an orthorhombic solid solution was found.

Regarding the $C_{12}A_7$-$Na_2O$ solid solution, it was found that its composition closely resembles that of the $C_3A$-$Na_2O$ system, and there is alsoa potential for forming solid solutions with cubic symmetry. When the $Na_2O$ content in the $C_{12}A_7$ solid solution reached approximately 8 %, a significant reduction in the unit cell size was observed from 12.0191 Å (at 1.8 wt. % $Na_2O$) to 11.9975 Å [16, 17].

Alkali metal admixtures can influence crystallisation processes, alter thermal stability, and promote the formation of specific polymorphic modifications of $C_3A$. However, the mechanism of this influence and its impact on subsequent hydration remain insufficiently understood. In this context, the present study focuses on investigating the effect of sodium and rubidium ions on the structure and formation of polymorphic modifications of $C_3A$ synthesised under laboratory conditions. A particular attention is paid to how the presence of these ions affects the hydration behaviour of the modified $C_3A$, with the aim of elucidating the relationship between crystal structure, chemical composition, and hydration reactivity.

## 2. Materials and methods

### 2.1. Raw material mixture composition

Calcium carbonate ($CaCO_3$, p.a. purity 99.0 %, Penta, Prague, Czech Republic), aluminium oxide ($Al_2O_3$. p.a. purity 98.5 %, Penta, Prague, Czech Republic), sodium carbonate ($Na_2CO_3$, p.a. purity 99.0 %, Penta, Prague, Czech Republic), and rubidium carbonate ($Rb_2CO_3$, p.a. purity 99.8 %, Sigma-Aldrich, USA) were used as precursors for the synthesis of tricalcium aluminate. The amount of raw materials was determined using stoichiometric calculations based on the molar ratio of atoms in the tricalcium aluminate ($C_3A$; $Ca_3Al_2O_6$), i.e. 3:2:6 (Ca:Al:O) as shown in Tables 2 and 3. In the presence of sodium or rubidium, this ratio was adjusted to take into account the substitution of the $Ca^{2+}$ ion by two $Na^+$ or $Rb^+$ ions in the $C_3A$ structure. The calculations took into account the molar masses of the elements and the compounds used, since their carbonate forms ($CaCO_3$ and $Na_2CO_3$) were used instead of calcium and sodium oxide.

The mixtures were homogenised by wet grinding in a laboratory planetary mill (Pulverisette 6, Fritsch, Idar-Oberstein, Germany). A 500 ml steel capsule

| $Na_2O$ [%] | $CaCO_3$ [g] | $Al_2O_3$ [g] | $Na_2CO_3$ [g] |
|---|---|---|---|
| 0.0 | 111.940 | 38.060 | 0.000 |
| 0.5 | 111.092 | 38.047 | 0.861 |
| 1.0 | 110.244 | 38.035 | 1.721 |
| 1.5 | 109.396 | 38.023 | 2.581 |
| 2.0 | 108.549 | 38.010 | 3.440 |
| 2.5 | 107.703 | 37.998 | 4.299 |
| 3.0 | 106.857 | 37.986 | 5.157 |
| 3.5 | 106.012 | 37.973 | 6.015 |
| 4.0 | 105.167 | 37.961 | 6.872 |
| 4.5 | 104.323 | 37.949 | 7.728 |

Table 2. Composition of raw material mixture for the preparation of $C_3A$ doped with $Na_2O$.

| $Rb_2O$ [%] | $CaCO_3$ [g] | $Al_2O_3$ [g] | $Rb_2CO_3$ [g] |
|---|---|---|---|
| 0.0 | 22.935 | 7.605 | 0.000 |
| 0.5 | 22.289 | 7.587 | 0.124 |
| 1.0 | 22.183 | 7.569 | 0.248 |
| 1.5 | 22.073 | 7.551 | 0.376 |
| 2.0 | 21.969 | 7.533 | 0.498 |
| 2.5 | 21.860 | 7.515 | 0.625 |
| 3.0 | 21.764 | 7.499 | 0.737 |
| 3.5 | 21.661 | 7.482 | 0.857 |
| 4.0 | 21.558 | 7.464 | 0.978 |
| 4.5 | 21.456 | 7.447 | 1.097 |

Table 3. Composition of raw material mixture for the preparation of $C_3A$ doped with $Rb_2O$.

with 20 mm diameter grinding media was used for the homogenisation of the sodium material mixture, while a smaller 80 ml capsule with 10 mm diameter grinding media was used for rubidium. The grinding was carried out at a speed of 350 rpm for 15 minutes. The samples were then dried at 105 °C for 24 hours in a laboratory oven (Binder C170, Binder GmbH., Tuttlingen, Germany).

The firing was carried out in a laboratory, high-temperature superkanthal furnace (2017S, Clasic CZ s.r.o., Řevnice, Czech Republic) in two phases: calcination at 1 000 °C (1 h, 8 $°C\,min^{-1}$) and then sintering at 1 350 °C (2 h, 8 $°C\,min^{-1}$). After firing, the samples were cooled by air flow and ground, first in a vibratory disc mill (RS 200. Retsch, Haan, Germany) at 1 000 rpm for 30 s, and then in a laboratory mill (McCrone Micronising Mill, Glen Creston, London, UK) for 150 s with 15 ml of isopropyl alcohol, in order to achieve the required fineness for X-ray analysis.

### 2.2. X-ray fluorescence analysis (XRF)

The chemical composition of the samples was verified by X-ray fluorescence spectrometry (XRF) on a 2.4 kW sequential wave-dispersive spectrometer (PANalytical Axios B.V., Alelo, the Netherlands) with an X-ray tube with a rhodium anode. The samples used for the analysis were borate tablets prepared by melting in a LeNeo Claisse electric melting unit at a temperature of 1 065 °C using a mixed flux of $Li_2B_4O_7$ and $LiBO_2$ in a flux/sample ratio of 15:1. The measured data were evaluated by SUPERQ V4.0 software. The values shown represent the average of three independent measurements.

### 2.3. X-ray diffraction analysis (XRD)

X-ray diffraction (XRD) analysis was performed on a diffractometer (XRD, Panalytical Empyrean B.V., Alelo, the Netherlands). The device operated in the Bragg-Brentano reflection geometry $\theta$-$\theta$ with parafocusing and was equipped with an X-ray tube with a copper anode ($\lambda = 1.54184$ Å), programmable divergent slits and a PIXcel3D detector with 255 active channels. The X-ray generator settings were 45 kV and 40 mA. The measured angular range was 5–80° with a step of 0.013° and a measurement time of 38 s per step. Each sample was measured four times, and the obtained records were then simply summed. The total measurement time per sample was 60 minutes. The Panalytical HighScore 3 plus software was used to identify individual phases. A qualitative analysis of the diffraction records was performed based on the ICSD database (2012 edition). Crystallite size was quantified and estimated using the Rietveld method and HighScore Plus software.

### 2.4. Isothermal calorimetry

The early hydration process of cement pastes with a water coefficient $\frac{w}{c} = 0.4$ was monitored by isother-

| | $Na_2O$ | $Al_2O_3$ | MgO | SiO2 | CaO | $Fe_2O_3$ | Others |
|---|---|---|---|---|---|---|---|
| 4 % $Na_2O$ | 4.105 | 35.001 | 0.192 | 0.168 | 59.433 | 0.125 | 0.976 |

TABLE 4. XRF analysis of $C_3A$ containing 4 % $Na_2O$.

| $Na_2O$ [%] | $C_3A$ cub | $C_3A$ ort | CaO | Mayenit | $C_3A$ cub | $C_3A$ ort | Cub/ort |
|---|---|---|---|---|---|---|---|
| 0.0 | 91.9 | 0.00 | 3.2 | 4.9 | 100 | 0.0 | 0.00 |
| 0.5 | 87.8 | 4.8 | 3.1 | 4.3 | 95.0 | 5.0 | 19.00 |
| 1.0 | 87.1 | 4.1 | 3.8 | 5.0 | 95.7 | 4.3 | 22.02 |
| 1.5 | 78.5 | 10.4 | 2.7 | 8.3 | 87.9 | 11.6 | 7.58 |
| 2.0 | 82.8 | 9.1 | 2.6 | 5.6 | 90.0 | 10.0 | 9.00 |
| 2.5 | 79.2 | 12.0 | 1.8 | 6.9 | 86.3 | 13.7 | 6.30 |
| 3.0 | 75.1 | 17.8 | 3.7 | 3.4 | 78.4 | 21.6 | 3.63 |
| 3.5 | 64.1 | 22.1 | 5.8 | 8.0 | 71.6 | 28.4 | 2.50 |
| 4.0 | 37.6 | 49.8 | 6.8 | 5.8 | 38.0 | 62.0 | 0.61 |
| 4.5 | 34.2 | 53.0 | 6.8 | 6.0 | 34.8 | 65.2 | 0.53 |

TABLE 5. Percentage of individual minerals in $C_3A$ samples containing $Na_2O$ determined by XRD analysis.

mal calorimetry using a TAM Air 8 device. Samples with a content of 0 %, 3 %, and 4.5 % of $Na_2O$ and $Rb_2O$ were used for the experiment. The heat flow and the total development of the heat of hydration were monitored for 7 days at a constant temperature of 25 °C. For the measurement, 0.5 g of the sample was weighed and poured into a 20 ml plastic ampoule. Mixing with deionised water took place ex situ for 2 minutes. Subsequently, the ampoule was immediately inserted into the calorimeter. The heat flow recording started exactly 3 minutes after the first contact of the sample with water. The deionised water was used as a reference material in an amount corresponding to the heat capacity of the paste.

## 3. RESULTS AND DISCUSSION

The results obtained in this study provide clear evidence of the different effects that $Na_2O$ and $Rb_2O$ have on the polymorphism and hydration behaviour of $C_3A$.

### 3.1. $NA_2O$ DOPANT

To verify the content of the used dopant after the calcination process, an XRF analysis was performed as indicated in Table 4. The aim was to determine whether there was any loss of sodium during the calcination process due to possible evaporation into the furnace atmosphere or other losses. The sample with the highest percentage content was selected, namely 4 % $Na_2O$.

The $Na_2O$ content in the sample remained constant, indicating that $Na_2O$ was successfully incorporated into the $C_3A$ structure.

An X-ray diffraction analysis was performed to characterize the phase composition of the synthesized tricalcium aluminate ($C_3A$) samples modified with different contents of sodium oxide ($Na_2O$) as shown in Table 5 and Figure 1. This analysis allowed to monitor the effect of $Na_2O$ addition on crystallinity and the presence of secondary phases, which can affect the reactivity and hydration behaviour of $C_3A$. By comparing the diffractograms of individual samples, it was possible to identify changes in the phase composition depending on the increasing $Na_2O$ content and to assess the degree of substitution or formation of sodium-stabilised phases.

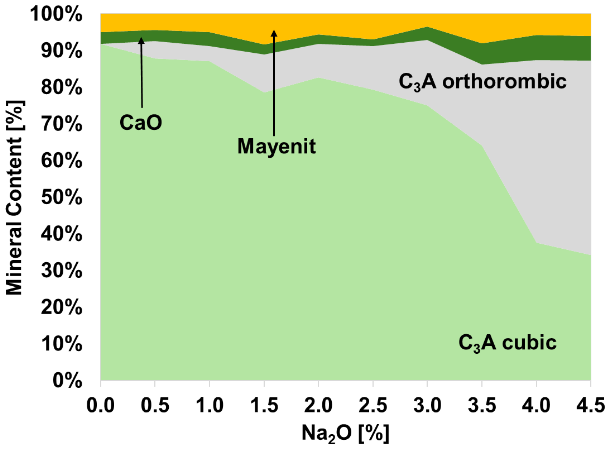

FIGURE 1. Graphical representation of the amount of individual minerals depending on the $Na_2O$ content.

The columns "$C_3A$ cub", "$C_3A$ ort" and "cub/ort" represent values normalised exclusively within the $C_3A$ phase. These values were calculated by subtracting the proportions of the remaining minerals from the total $C_3A$ content and subsequently recalculating the relative amounts of the individual polymorphs within this phase. Therefore, they do not directly correspond to columns 2–3, which report absolute phase abundances in the whole sample. These values are normalised within the $C_3A$ phase based on a separate Rietveld refinement.

The results of the X-ray diffraction (XRD) analysis indicate that at low sodium concentrations of

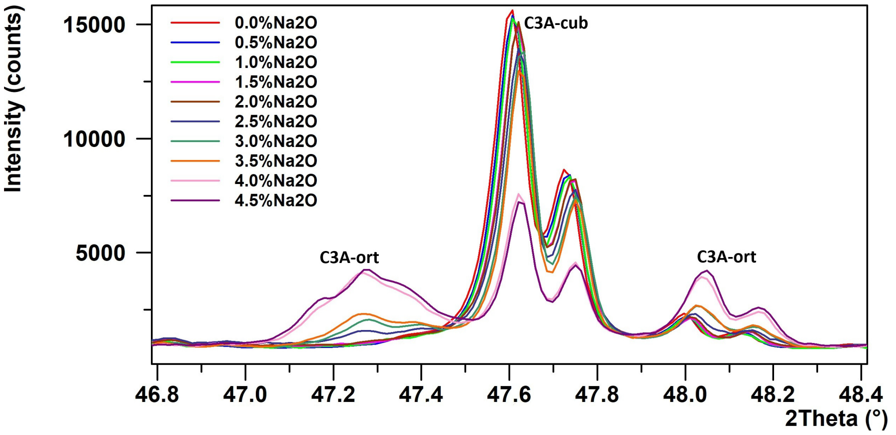

Figure 2. Detail of the area between 46.8 and 48.4 $2\theta$.

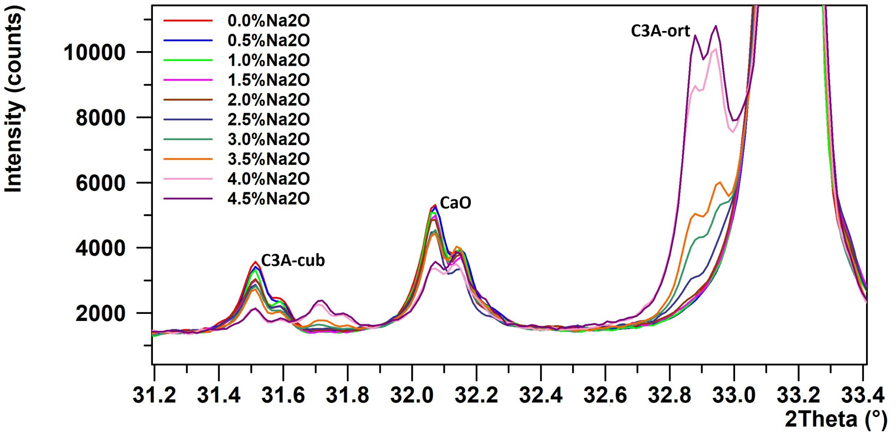

Figure 3. Detail of the area between 31.2 and 33.4 $2\theta$.

0–2.5 wt. %, stabilisation of the cubic $C_3A$ modification occurs. This phenomenon is consistent with previous studies [2], which report that alkaline ions, particularly $Na^+$, can promote the formation of the cubic phase through their interaction with the aluminate structure. At $Na_2O$ contents of up to approximately 2.5 wt. %, the stabilisation of cubic $C_3A$ observed in this work is consistent with the findings of Takeuchi and Nishi [7] and Lee et al. [8], who showed that low alkali concentrations promote cubic symmetry through partial filling of vacancies within the $Al_6O_{18}$ rings. In our case, this stabilisation is reflected in the high proportion of cubic $C_3A$ and low CaO residues, indicating an effective incorporation of $Na^+$ into the structure without significant lattice distortion. However, upon increasing the $Na_2O$ content to 3–4.5 wt. %, a gradual increase in the intensity of diffraction reflections corresponding to the orthorhombic $C_3A$ modification was observed. This trend suggests that higher sodium dopant concentrations destabilise the cubic phase and support its transformation into the orthorhombic form.

The critical point of phase transformation was identified at approximately 4 wt. % $Na_2O$, where the orthorhombic phase begins to dominate. This shift is clearly documented in Figures 2 and 3, which show a decline in the intensity of the cubic phase diffraction peaks in favour of orthorhombic ordering. It is likely that sodium at higher concentrations induces local lattice distortions, contributing to the crystallochemical instability of the cubic $C_3A$. At higher $Na_2O$ levels (3–4.5 wt. %), the shift towards the orthorhombic modification follows the phase evolution sequence described by Ostrowski and Żelazny [15], although the transformation threshold appears slightly lower in our study. While the crystallographic evidence of the monoclinic form reported above 5.2 wt. % in [15] did not emerge here, the dominance of orthorhombic $C_3A$ at 4 wt. % $Na_2O$ aligns with the hypothesis that synthetic conditions, especially firing temperature, diffusion rates, and melt homogeneity, can shift polymorphic stability fields. The concurrent increase in free CaO and mayenite at higher $Na_2O$ contents also agrees with the work of Lee et al. [8] and Fukuda et al. [6], who found that excessive sodium preferentially forms Na-Al-O complexes and inhibits complete incorporation of CaO into the $C_3A$ phase.

Samples with higher $Na_2O$ content exhibited an increased amount of free CaO, as evidenced by the diffraction data shown in Figure 4. This phenomenon can be explained by the preferential reaction of $Na_2O$ with $Al_2O_3$, leading to the formation of sodium-aluminate phases and leaving part of the lime unbound.

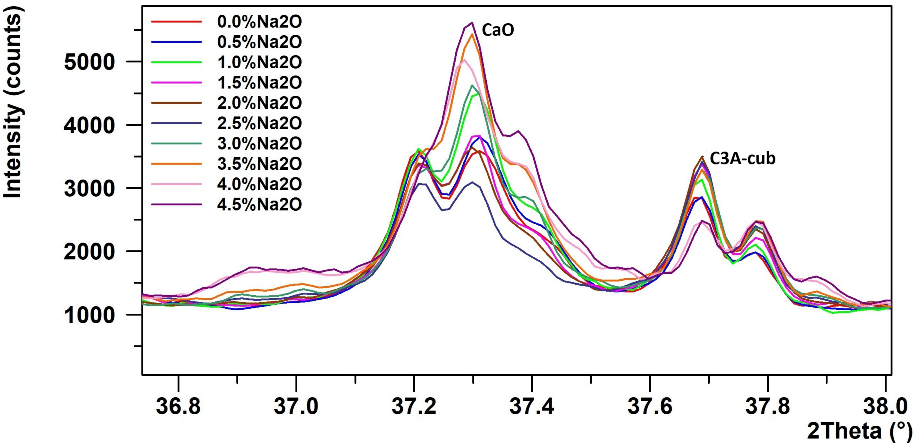

Figure 4. Detail of the area between 36.8 and 38.0 2θ.

| | $Rb_2O$ | $Al_2O_3$ | MgO | SiO2 | CaO | $Fe_2O_3$ | Others |
|---|---|---|---|---|---|---|---|
| 4 % $Rb_2O$ | 1.529 | 35.065 | 0.203 | 0.253 | 61.583 | 0.208 | 1.159 |

Table 6. XRF analysis of $C_3A$ containing 4 % $Rb_2O$.

The detection of mayenite ($Ca_{12}Al_{14}O_{33}$) in all samples, particularly in those with higher dopant levels, serves as an indicator of calcium saturation in the system and the presence of free CaO. Since mayenite primarily forms under conditions of CaO excess and low $SiO_2$ activity, its occurrence can be considered a consequence of limited silicon availability and excess lime. This finding is significant, as the presence of mayenite can influence the hydration behaviour of cementitious phases and thus the final mechanical properties of the resulting material.

In summary, the sodium dopant has a substantial effect on the stability of crystallographic forms of $C_3A$, and its concentration dictates the direction of phase transformation between the cubic and orthorhombic modifications. In addition, sodium plays a crucial role in the reactivity of the system during clinkering and in the final mineralogy of the product.

### 3.2. $Rb_2O$ DOPANT

Analogously to sodium, the XRF analysis was performed to verify whether the required percentage of the second dopant in the form of $Rb_2O$ remained in the sample after the calcination process (see Table 6). A sample containing 4 % dopant was selected.

The results indicate that some of the $Rb_2O$ was probably lost by evaporation into the furnace atmosphere during the high-temperature firing, which can be attributed to the high volatility of rubidium compounds under the given conditions. This phenomenon could lead to lower doping efficiency and affect the resulting phase composition and structural parameters of the prepared $C_3A$. This was reflected in the absence of significant diffraction lines corresponding to rubidium compounds in the subsequent X-ray diffraction XRD analysis results.

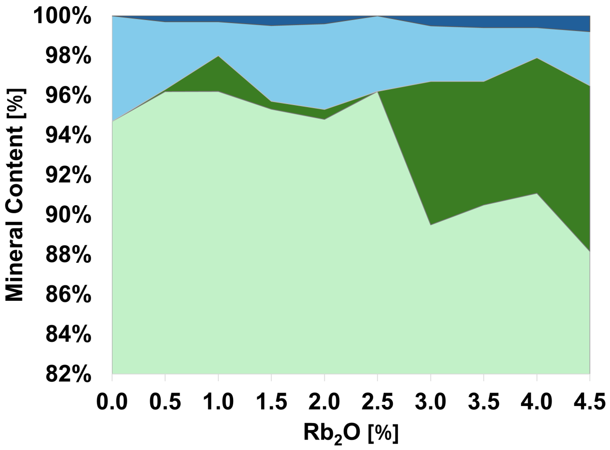

Figure 5. Graphical representation of the amount of individual minerals depending on the $Rb_2O$ content.

The X-ray diffraction analysis of samples doped with rubidium oxide $Rb_2O$ (see Figure 5 and Table 7) showed that at dopant concentrations ranging from 0 to 2.5 wt. %, only the cubic modification of tricalcium aluminate $C_3A$ was detected, along with phases of portlandite ($Ca(OH)_2$), mayenite ($Ca_{12}Al_{14}O_{33}$), and unreacted lime (CaO). The absence of other crystallographic modifications of $C_3A$, especially the orthorhombic form, indicates that rubidium was not incorporated into the crystal structure of this phase.

Rubidium as a dopant apparently did not enter the $C_3A$ lattice due to its relatively large ionic radius ($Rb^+ \approx 1.52$ Å), which significantly exceeds the size of commonly substituted alkaline cations such as $Na^+$ (1.02 Å) or $K^+$ (1.38 Å). This difference in ionic radius and polarisability makes rubidium crystallochemically incompatible for substitution in the $C_3A$ structure, as also confirmed by previous literature studies on alkali-doped aluminate phases.

| $Rb_2O$ [%] | $C_3A$ cub | CaO | Mayenit | Portlandite |
|---|---|---|---|---|
| 0.0 | 94.7 | 0.0 | 5.3 | 0.0 |
| 0.5 | 96.1 | 0.1 | 3.4 | 0.3 |
| 1.0 | 96.2 | 1.8 | 1.7 | 0.3 |
| 1.5 | 95.4 | 0.4 | 3.8 | 0.5 |
| 2.0 | 94.7 | 0.5 | 4.3 | 0.4 |
| 2.5 | 96.2 | 0.0 | 3.8 | 0.0 |
| 3.0 | 89.5 | 7.2 | 2.8 | 0.5 |
| 3.5 | 90.5 | 6.2 | 2.7 | 0.6 |
| 4.0 | 91.0 | 6.8 | 1.5 | 0.6 |
| 4.5 | 88.0 | 8.3 | 2.7 | 0.8 |

Table 7. Percentage of individual minerals in $C_3A$ samples containing $Rb_2O$ determined by XRD analysis.

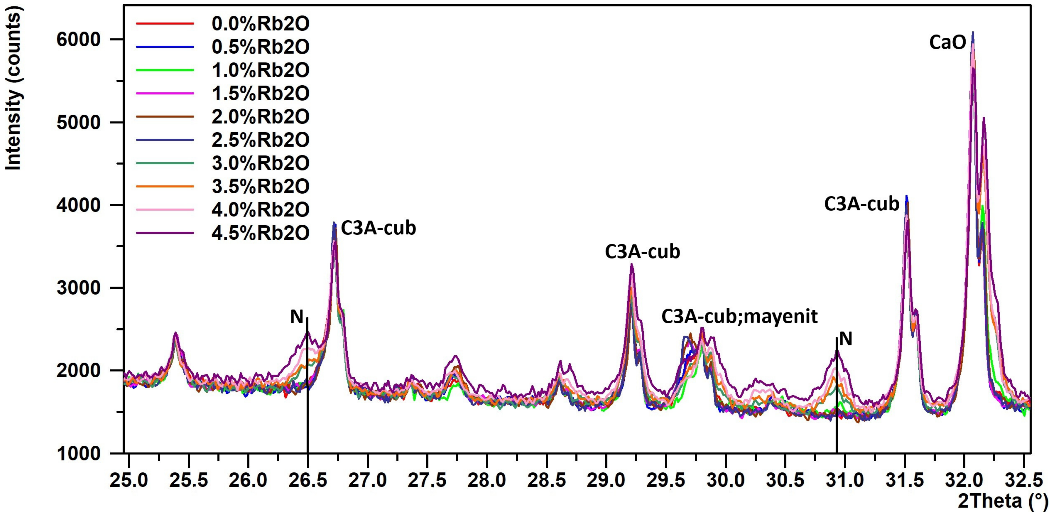

Figure 6. Detail of the area between 25.0° and 32.5° 2θ($N$-unknown phase).

Although no structural changes were observed within the $C_3A$ phase itself, unidentified reflections were recorded in the diffractograms, which might be related to the formation of secondary rubidium-containing compounds. These phases occur in minor amounts and have not yet been conclusively identified, see Figure 6. Their formation could result from rubidium segregation during the firing, suggesting limited reactivity of this element in the $CaO$-$Al_2O_3$ system.

Similarly to sodium-doped samples, an increased amount of residual lime was observed in the system with higher $Rb_2O$ concentration 3–4.5 wt. %. This phenomenon is evident from both the overall phase quantification and from the detailed analysis of the intensity of the CaO diffraction peaks, see Figure 7, which show a clearly higher intensity in samples prepared in the second production batch. The probable cause is either the lower reactivity of rubidium-modified systems, leading to an incomplete lime transformation during firing, or changes in the melting and crystallisation dynamics during the synthesis caused by the presence of highly electrostatic $Rb^+$ ions, which could have influenced ion diffusion in the melt. From the perspective of the phase stability of $C_3A$, rubidium can be considered a passive, non-structural dopant that may influence the overall mineralogy of the system through the formation of secondary, yet unidentified phases, but does not significantly interact with the main clinker components. Its presence thus provides important insights not only into the limits of ionic substitution in Portland clinker phases, but also into the reactivity and complexity of interactions in systems modified by alkali metal elements.

### 3.3. Isothermal calorimetry

Samples were selected for hydration testing in an isothermal calorimeter over a period of 7 days. These included a reference sample without dopants, as well as samples containing 3 % and 4.5 % of sodium oxide or rubidium oxide (see Figures 8 and 9).

The highest thermal response during the initial hydration phase was observed for the sample containing 4.5 % $Na_2O$, which showed a sharp increase in the heat released during the first 24 hours, reaching a maximum value of approximately $800\,\mathrm{J\,g^{-1}}$. After a slight decrease, a further increase followed, while the value of the heat released remained stable for the rest of the monitored period. Conversely, the lowest thermal response was observed for the sample doped with 3 % $Rb_2O$, for which the value of the heat released was around $300\,\mathrm{J\,g^{-1}}$, with a very gradual increase in time.

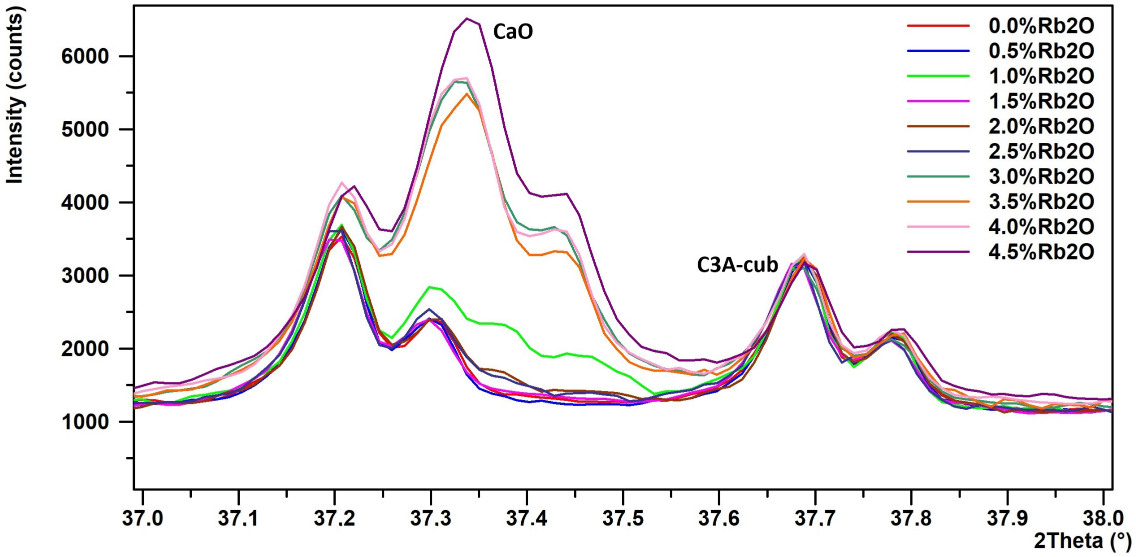

FIGURE 7. Detail of the area between 37.0° and 38.0° 2θ.

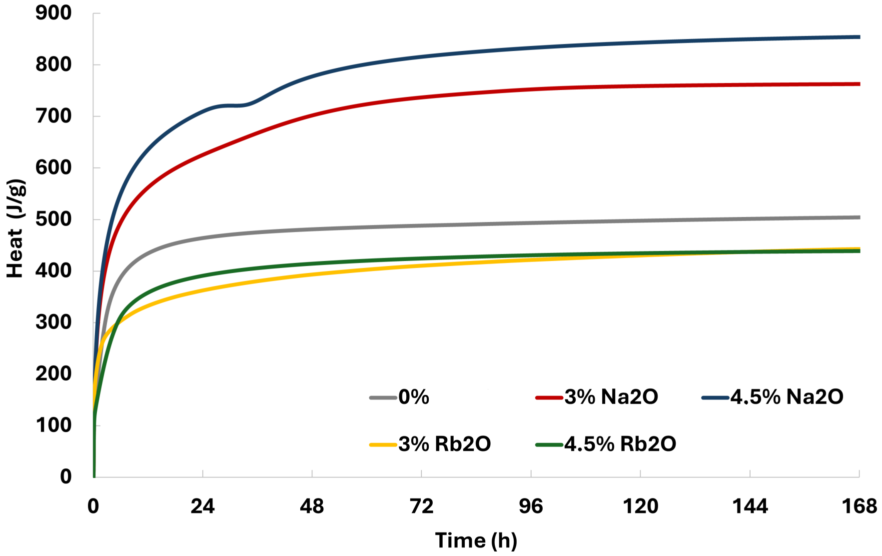

FIGURE 8. Time dependence of heat development during $C_3A$ hydration.

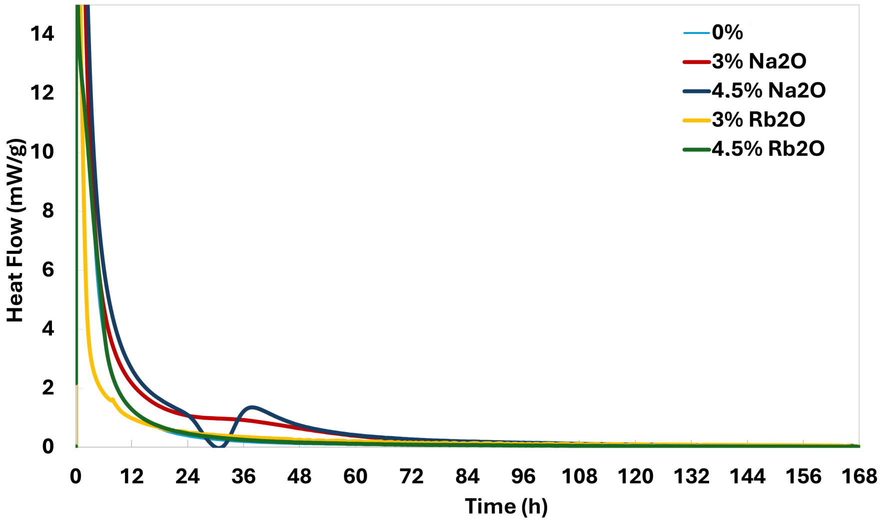

FIGURE 9. Dependence of heat flow on the length of the hydration time.

The hydration retardation observed in $Rb_2O$-doped samples have no direct counterpart in the literature, but it is reasonable to attribute this behaviour to the presence of these segregated Rb-containing phases, which likely inhibit the dissolution of $C_3A$ or block reactive surfaces. This contrasts sharply with $Na_2O$, which enhances the dissolution and accelerates hydration. The retarding effect of rubidium, therefore, represents a new and previously unreported behaviour among alkali dopants in $C_3A$. The reference sample without the addition of alkalis showed a steep increase in the heat released during the first 24 hours, but the maximum value did not exceed $450\,\mathrm{J\,g^{-1}}$, and subsequently remained constant. A similar course was observed for the sample with 4.5 % $Rb_2O$, but with an even lower level of heat released. Based on these results, it can be stated that samples with a higher $Na_2O$ content show higher reactivity, which is manifested by a more intense development of the heat of hydration. This effect is probably associated with a faster formation of hydrated phases, especially of the AFm type. Conversely, the presence of $Rb_2O$ has a retarding effect on hydration, which is reflected in a lower and slower heat evolution. The different behaviour of sodium and rubidium in the system thus points to their different influence on the kinetics of hydration of tricalcium aluminate.

It is clear from the heat flow measurements that during the first 12 hours after the start of hydration, a steep increase occurred for all samples, which corresponds to the exothermic reaction associated with the initial hydration of $C_3A$. Fluctuations in heat flow were recorded for the sample containing 4.5 % $Na_2O$, the cause of which was not clearly identified, but may be related to unstable formation of intermediates or fluctuations in reaction kinetics. After 72 hours, zero heat flow was recorded in all $Na_2O$-doped samples, which indicates the end of the main hydration phase. The reference sample and the sample containing 4.5 % $Rb_2O$ also showed a rapid onset of hydration in the first 12 hours, but the subsequent decrease in heat flow occurred more slowly and zero value was reached only after approximately 48 hours. This difference in heat flow confirms that the presence of sodium accelerates hydration processes, while rubidium has an inhibitory effect, which corresponds to the results of the total heat released and the observed phase evolution.

The calorimetry results further support these structural observations. As documented by Joseph et al. [11] and Hirsch et al. [12], orthorhombic $C_3A$ exhibits higher dissolution rates and greater early exothermicity compared with cubic $C_3A$. The significantly higher heat release of $Na_2O$-rich samples in this study is, therefore, consistent with the literature, even in the absence of sulphates.

## 4. Conclusion

The results of this study align with previously published data on sodium-doped $C_3A$, corroborating known mechanisms of structural substitution and hydration acceleration. At the same time, they expand the current understanding of alkali-aluminate interactions by revealing the crystallochemical incompatibility of rubidium with $C_3A$, its inability to form stable solid solutions, and its inhibitory influence on hydration kinetics.

- The addition of $Na_2O$ and $Rb_2O$ had a major impact on the polymorphic composition of $C_3A$ and its hydration behaviour.
- $Na_2O$ is successfully incorporated into the $C_3A$ structure.
- Up to a content of 2.5 %, the cubic polymorph predominates.
- At higher concentrations, a transition to orthorhombic $C_3A$ occurs.
- $Rb_2O$ demonstrated low compatibility with the $C_3A$ structure.
- The reason is probably the larger ionic and atomic radius of rubidium compared to calcium.
- New, yet unidentified phases are formed.
- During firing, significant losses of $Rb_2O$ occur due to its evaporation.
- Samples with a higher $Na_2O$ content showed increased reactivity due to orthorhombic $C_3A$, which has a higher hydration rate.
- Samples containing $Rb_2O$ showed a slowdown in hydration, the cause of which is not yet clear.

## Acknowledgements

We acknowledge the financial support of Czech Science Foundation under the project “The role of combination of fluxes, mineralizers and SCMs on properties of low-energy clinker” (23-05122S).

## References

[1] S. P. Varma, C. D. Wall. A monoclinic tricalcium aluminate ($C_3A$) phase in a commercial Portland cement clinker. *Cement and Concrete Research* **11**(4):567–574, 1981. `https://doi.org/10.1016/0008-8846(81)90086-7`

[2] H. F. W. Taylor. *Cement chemistry.* Thomas Telford, London, UK, 2nd edn., 1997. ISBN 0-7277-2592-0.

[3] A. Wesselsky, O. M. Jensen. Synthesis of pure Portland cement phases. *Cement and Concrete Research* **39**(11):973–980, 2009. `https://doi.org/10.1016/j.cemconres.2009.07.013`

[4] P. C. Hewlett (ed.). *Lea’s chemistry of cement and concrete.* Elsevier, Oxford, UK, 4th edn., 1998.

[5] P. Barnes, J. Bensted. *Structure and performance of cements.* CRC Press, 2nd edn., 2002. ISBN 9780429178429.

[6] K. Fukuda, S. Inoue, H. Yoshida. Cationic substitution in tricalcium aluminate. *Cement and Concrete Research* **33**(11):1771–1775, 2003. `https://doi.org/10.1016/S0008-8846(03)00172-8`

[7] Y. Takéuchi, F. Nishi. Crystal-chemical characterization of the $3\,CaO \cdot Al_2O_3$-$Na_2O$ solid-solution series. *Zeitschrift Fur Kristallographie* **152**(1–4):259–308, 1980. `https://doi.org/10.1524/zkri.1980.152.14.259`

[8] F. C. Lee, H. M. Banda, F. P. Glasser. Substitution of Na, Fe and Si in tricalcium aluminate and the polymorphism of solid solutions. *Cement and Concrete Research* **12**(2):237–246, 1982. `https://doi.org/10.1016/0008-8846(82)90010-2`

[9] K. Fukuda, S. Inoue, H. Yoshida. Substitution of sodium and silicon in tricalcium aluminate. *Journal of the American Ceramic Society* **86**(1):112–114, 2003. `https://doi.org/10.1111/j.1151-2916.2003.tb03286.x`

[10] D. Axthammer, T. Lange, J. Dengler, T. Gädt. Early hydration and viscoelastic properties of tricalcium aluminate pastes influenced by soluble sodium salts. *Cement and Concrete Research* **190**:107788, 2025. `https://doi.org/10.1016/j.cemconres.2025.107788`

[11] S. Joseph, J. Skibsted, Ö. Cizer. A quantitative study of the $C_3A$ hydration. *Cement and Concrete Research* **115**:145–159, 2019. `https://doi.org/10.1016/j.cemconres.2018.10.017`

[12] T. Hirsch, T. Matschei, D. Stephan. The hydration of tricalcium aluminate ($Ca_3Al_2O_6$) in Portland cement-related systems: A review. *Cement and Concrete Research* **168**:107150, 2023. `https://doi.org/10.1016/j.cemconres.2023.107150`

[13] X. Liu, P. Feng, C. Lyu, S. Ye. The role of sulfate ions in tricalcium aluminate hydration: New insights. *Cement and Concrete Research* **130**:105973, 2020. `https://doi.org/10.1016/j.cemconres.2020.105973`

[14] J. S. Andrade Neto, P. R. de Matos, A. G. De la Torre, et al. The role of sodium and sulfate sources on the rheology and hydration of $C_3A$ polymorphs. *Cement and Concrete Research* **151**:106639, 2022. `https://doi.org/10.1016/j.cemconres.2021.106639`

[15] C. Ostrowski, J. Żelazny. Solid solutions of calcium aluminates $C_3A$, $C_{12}A_7$ and CA with sodium oxide. *Journal of Thermal Analysis and Calorimetry* **75**(3):867–885, 2004. `https://doi.org/10.1023/B:JTAN.0000027182.40442.fe`

[16] D. Knudsen, G. A. Peterson, P. F. Pratt. Lithium, sodium, and potassium. In A. L. Page (ed.), *Methods of Soil Analysis: Part 2 Chemical and Microbiological Properties*, pp. 225–246. John Wiley & Sons, Ltd, 1982. `https://doi.org/10.2134/agronmonogr9.2.2ed.c13`

[17] J. H. Ideker, K. L. Scrivener, H. Fryda, B. Touzo. 12 – Calcium aluminate cements. In P. C. Hewlett, M. Liska (eds.), *Lea's Chemistry of Cement and Concrete*, pp. 537–584. Butterworth-Heinemann, 5th edn., 2019. `https://doi.org/10.1016/B978-0-08-100773-0.00012-5`